Chemical Geology, 109 (1993) 125–134
Elsevier Science Publishers B.V., Amsterdam

[EW]

Major-element ratios in synthetic fluid inclusions by synchrotron X-ray fluorescence microprobe

David A. Vanko[a], Stephen R. Sutton[b], Mark L. Rivers[b] and Robert J. Bodnar[c]
[a]*Department of Geology, Georgia State University, Atlanta, GA 30303, USA*
[b]*Department of the Geophysical Sciences, University of Chicago, Chicago, IL 60637, USA*
[c]*Department of Geological Sciences, Virginia Polytechnic Institute and State University, Blacksburg, VA 24061, USA*

(Received November 4, 1992; revised and accepted January 24, 1993)

ABSTRACT

Individual fluid inclusions in quartz were investigated by synchrotron radiation X-ray fluorescence (SXRF) microprobe to develop protocols for major-element microanalysis. Studies were conducted of synthetic fluid inclusions in Brazilian quartz that contain fluids of known NaCl–$CaCl_2$–H_2O and KCl–H_2O compositions. Inclusions were irradiated by synchrotron X-rays and the resulting energy-dispersive spectra were corrected for fluorescence yield and absorption effects to obtain Ca/Cl and K/Cl ratios. Results are commonly better than ±30% relative to the nominal ratio. Element ratios obtained by SXRF may be combined with results of heating and freezing studies to characterize non-destructively the bulk major-element composition of individual inclusions. Extension of the analytical protocol to elements of higher atomic number (e.g., trace and transition elements) will result in better precision as absorption effects and peak overlaps become less problematic.

1. Introduction

As new and more sophisticated microanalytical techniques are applied to fluid inclusion studies, our ability to obtain more reliable quantitative information on inclusion composition continues to improve [cf. the review by Roedder (1990)]. Each technique has its strengths and drawbacks, and no single method has yet been identified that can provide a comprehensive characterization of a fluid inclusion. One recently developed method is non-destructive, sensitive enough to detect major and trace elements with atomic numbers of 14 (Si) and above, and operates as a microprobe, with beam diameters of the order of 10 μm. This is the synchrotron radiation X-ray fluorescence (SXRF) microprobe (Bassett and Brown, 1990; Chen et al., 1990; Rivers et al., 1991), in which high-intensity X-rays are tapped from an electron storage ring and directed onto a fluid inclusion. The resulting characteristic fluorescence spectrum reveals the elements and their concentrations within the inclusion (Fig. 1).

The SXRF microprobe provides multi-element chemical analyses that lack only the lightest elements ($Z \leqslant 13$). Combined with a freezing study that reveals the bulk salinity of the same inclusions, well-constrained fluid compositions may be calculated. In this paper, we report experiments performed at the National Synchrotron Light Source (NSLS) of Brookhaven National Laboratory (BNL), Upton, New York, U.S.A. We investigated synthetic fluid inclusions in natural quartz that contain $H_2O \pm CaCl_2 \pm NaCl \pm KCl$. We present determinations of Ca/Cl and K/Cl ratios and assess the effects of variable inclusion depth, size, geometry and salinity on those estimates. Our results show that these elemental ratios can be determined to better than ±30%,

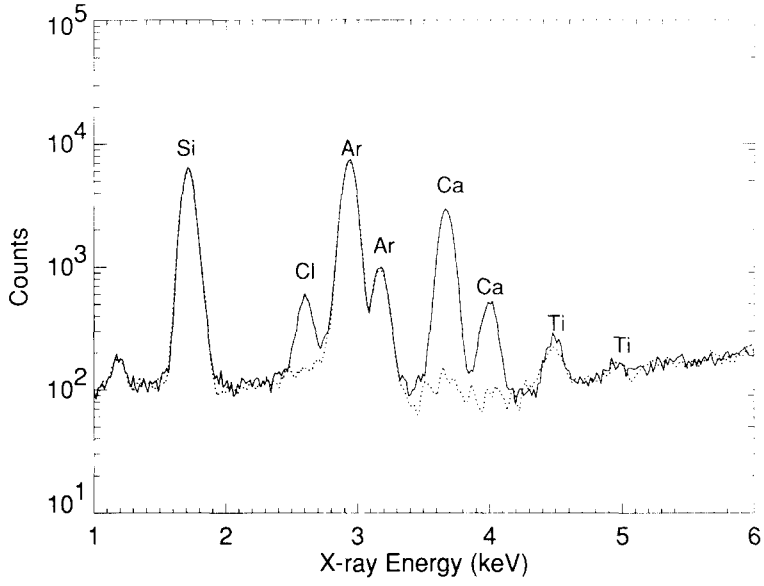

Fig. 1. Synchroton X-ray fluorescence spectrum of a synthetic $NaCl–CaCl_2–H_2O$ fluid inclusion in quartz. Two spectra are overlain: one of the fluid inclusion (*solid line*) and one of "background" quartz several tens of μm away (*dotted line*). For both spectra, peaks for Si, Ar and Ti are identical, and derive from the host quartz and the air between sample and detector. There is no Na peak due to absorption effects. Peaks for Cl and Ca derive from the fluid inclusion. Spectra nsls*99.13* and nsls*99.16*. Acquisition time was 10 min.

but that higher precision may be realized when critical parameters such as inclusion depth are better constrained. Because we chose to focus here on the low-Z elements which are most heavily absorbed, we predict that application of our experimental protocol to studies of high-Z elements (e.g., transition metals) may yield similar or even better overall results.

2. Background and previous work

Synchrotron radiation is emitted when charged particles such as electrons or positrons are accelerated. In an electron storage ring, radiation is generated as electrons are guided with bending magnets around the curves of a closed loop. The white spectrum of the synchrotron radiation is characterized by high brilliance, a very narrow divergence and strong polarization parallel to the plane of the ring.

Synchrotron radiation is used in a variety of earth science applications (Bassett and Brown, 1990) and it is well suited for an X-ray fluorescence (XRF) microprobe because of the brightness and polarization of the beam (e.g., Chen et al., 1990). The brightness allows a fine beam (as small as 5 μm across) to have enough flux to generate sufficient fluorescent X-rays in the sample for trace-element analysis. The polarization allows a detector to be positioned in such a way as to reduce significantly the scattered background, thus improving signal-to-noise ratio and lowering detection limits. The SXRF microprobe has the advantage of high sensitivity, multi-element capability, non-destructive analysis and minimal sample preparation (Rivers et al., 1991). Various SXRF trace-element studies have been carried out on earth materials including ores (e.g., Chen et al., 1987), meteorites (Sutton et al., 1987; Treiman and Sutton, 1992), coals (White et al., 1989), stratospheric particles (e.g., Sutton and Flynn, 1990; Flynn and Sutton, 1992), carbonates (Kopp et al., 1990), feldspars (Lu et al., 1989), silicate melt inclusions (Lowen-

stern et al., 1991) and fluid inclusions (Frantz et al., 1988).

Frantz et al. (1988) conducted a pilot study at the Stanford Synchrotron Radiation Laboratory and at NSLS–BNL to demonstrate the utility of SXRF for analysis of fluid inclusions. Synthetic inclusions in quartz containing $CaCl_2$, $ZnCl_2$ and $MnCl_2$ were studied, and a thin glass standard from the U.S. National Bureau of Standards was used for quantification. Two fluid inclusion analyses gave 0.065 *M* $ZnCl_2$ for a synthetic inclusion containing 0.1 *M* $ZnCl_2$, and 0.093 *M* $MnCl_2$ for an inclusion containing 0.1 *M* $MnCl_2$. More recently, Rankin et al. (1992) reported elemental ratios for transition metals in natural topaz-hosted fluid inclusions.

3. Methods

Synthetic fluid inclusions were prepared using reagent grade starting materials and natural inclusion-free Brazilian quartz. The technique, described in full by Bodnar and Sterner (1987), involves fracturing a quartz core, drying it completely, loading it with the fluid components in a sealed Pt capsule, and annealing the quartz fractures at elevated *P* and *T*. The quartz is sectioned into 1-mm slices which are then polished on each side.

In the X-ray microprobe, characteristic radiation from heavier elements within inclusions is absorbed less than that from lighter elements, and these mass absorption effects limit the depth at which an inclusion may be examined. A practical limit for detecting characteristic *K*-series X-rays from light elements (e.g., Cl) seems to be of the order of 10 μm, whereas a practical limit for heavy elements (e.g., Zn) is more like 100 μm (Fig. 2). Consequently, only those inclusions within 10–15 μm of the upper surface and having a maximum dimension $\lesssim 12$ μm are chosen for study.

Depths are measured initially using the graduated fine focus knob of a Zeiss® WL microscope with a 40× or 50× objective. The measurements are refined with a confocal microscope system (Newport® Instruments Model VX100 mounted on an Olympus® BHT microscope, 40× total objective magnification) in reflected light. The measurements are repeated 8–12 times and an average apparent depth is assigned. Overall, we estimate this value to be accurate to $\sim \pm 1$ μm. The actual depth is the apparent depth times the index of refraction of quartz. Since the synthetic fluid inclusion chips are oriented with *c*-axis parallel to the light path, $n = 1.544$. Because of the sample geometry in the SXRF microprobe (Fig. 3), the actual quartz thickness traversed by incident and fluorescent X-rays is $d/\cos(45°)$, where d is the fluid inclusion depth.

The SXRF on beamline X26A at NSLS–BNL (Fig. 3) consists of beam shaping slits, an ion chamber for monitoring beam current, an X–Y–Z–θ specimen stage with ± 1-μm precision, an optical microscope and a solid-state Si(Li) detector (EDS system). Selected inclusions were irradiated for 5–30 min, with X-ray beams varying from ~ 10 to 25 μm. EDS spectra are accumulated in a 2048-channel multichannel analyzer. Elemental peak areas are identified and integrated with the aid of peak fitting routines, and the background-corrected counts for each element are then used to evaluate elemental concentrations.

One necessity in analyzing fluid inclusions by XRF is predicting accurately the generation efficiency of fluorescent X-rays and the absorption of X-rays by the fluid inclusion itself. These effects are calculated theoretically by modelling each inclusion as an infinite layer of homogeneous fluid between two quartz plates. Differences in the fluorescence efficiency and self-absorption for various elements are accounted for by calculating a theoretical yield, Y, using the program NRLXRF (Criss, 1977). Thus, the elemental ratio in the inclusion is related to the emitted X-ray intensities by:

$$X_a/X_b = (I_{0,a}/I_{0,b})/Y \qquad (1)$$

where X_a and X_b represent the concentration

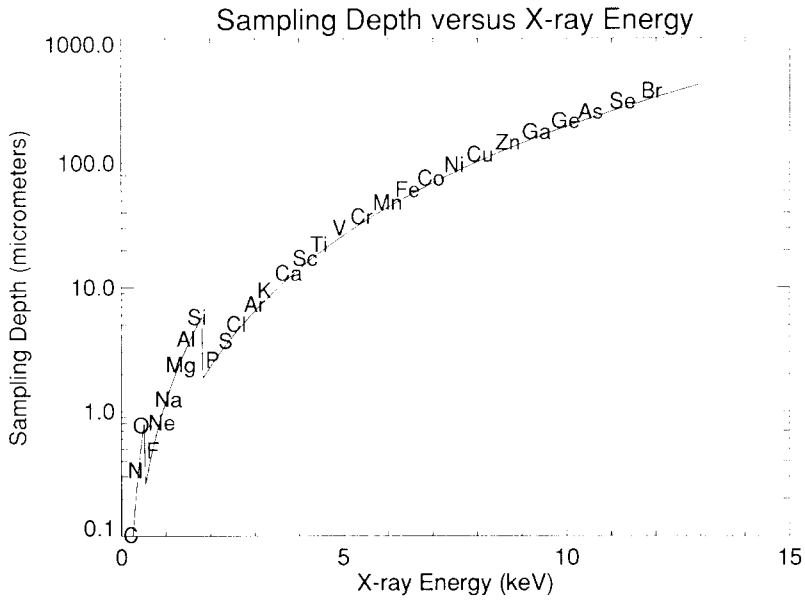

Fig. 2. Plot illustrating the effects of X-ray absorption by the quartz host. The sampling depth is defined as the thickness at which 37% (1/e) of the X-rays of a given energy, generated within a fluid inclusion, will successfully traverse the overlying quartz without being absorbed. Energies of characteristic radiation from elements of interest are labelled. The sampling depth can be used as a guide to the practical depth limit of inclusions in quartz that are amenable to SXRF analysis for that element. When interested in obtaining data on Cl, for instance, we limit our observations to inclusions within 10–15 μm of the sample surface. Studies of transition elements, in contrast, may involve much deeper inclusions.

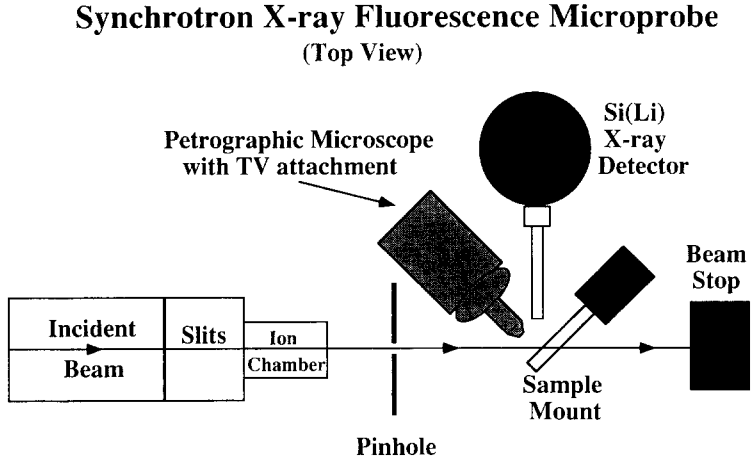

Fig. 3. Schematic of the synchrotron XRF microprobe at Brookhaven National Laboratory. Note that the specimen is oriented at 45° to the incoming X-ray beam.

of elements a and b, respectively; and I_0 is the X-ray intensity exiting the inclusion. For $NaCl–CaCl_2–H_2O$ inclusions varying from 1 to 10 μm thick and encompassing the range of compositions synthesized (35–65 wt% total salts), $Y=4.7\pm0.2$ (this value is specific to X26A at BNL because it depends on the shape of the exciting synchrotron X-ray spectrum). That is, fluorescent X-rays emerging from the top of an hypothetical inclusion containing a

1:1 ratio of Ca and Cl comprise 47 Ca-K_α X-rays for every 10 Cl-K_α X-rays. For our $CaCl_2$–H_2O inclusions varying from 5 to 42 wt% $CaCl_2$, $Y = 4.7 \pm 0.5$; and for the KCl–H_2O inclusions with 20 and 36 wt% KCl, the K/Cl yield factor is 3.0 ± 0.1. The yield factor is relatively insensitive to large variations in inclusion composition and to variations in inclusion thickness because, due to self-absorption, most fluorescent X-rays are generated near the top of the inclusion.

Another factor in analyzing inclusions by XRF is correcting accurately for X-ray absorption by the host mineral. The X-rays emerge from the fluid inclusions and must traverse a thickness of quartz before they can be detected. Mass absorption is defined by:

$$I/I_0 = \exp(-\mu z) \tag{2}$$

where I_0 is the X-ray intensity exiting the inclusion; I is the X-ray intensity exiting the quartz lid; μ is the mass absorption coefficient; and z is the thickness of quartz. For two elements,

$$I_{0,a}/I_{0,b} = I_a/I_b \, [\exp\{-z(\mu_a - \mu_b)\}]^{-1} \tag{3}$$

where a and b designate the two elements. For a quartz host, $\mu_{Ca} = 0.0885$ and $\mu_{Cl} = 0.22026$ (the units for these coefficients are μm^{-1} and we measure z in μm).

Further correction is necessary to account for differential absorption as X-rays traverse the air from the sample to the detector (typically 5 cm), and the 20-μm-thick Be window on the detector. A factor, A, of 1.078 is predicted for Ca and Cl, and this can be adjusted for sample-detector airpaths different from 5 cm.

The total correction required to recalculate an elemental ratio from the observed ratio of X-ray counts is:

$$X_a/X_b = (I_{0,a}/I_{0,b})/(YA)$$
$$= (I_a/I_b)/[YA \exp\{-z(\mu_a - \mu_b)\}] \tag{4}$$

and the equation we used for the ratio Ca/Cl is:

$$X_{Ca}/X_{Cl} = (I_{Ca}/I_{Cl})/[4.96 \exp(0.132z)] \tag{5}$$

An analogous equation can be written for any elemental ratio of interest (e.g., K/Cl, Cl/Br).

By assuming a single Y-value for inclusions with varying thickness and composition, we recognize an uncertainty in Y of $\pm 10\%$, leading to a comparable uncertainty in X_{Ca}/X_{Cl}. A more precise determination could result from refining the value of Y by iteration. However, uncertainty in the measured depth is a more severe limiting factor on determining X_{Ca}/X_{Cl}. A variation of $\pm 1\,\mu m$ in the depth of an inclusion leads to an uncertainty of $\pm 20\%$ in the calculated X_{Ca}/X_{Cl} ratio. Significantly, the same depth variation leads to less than $\pm 10\%$ uncertainty in the ratio between two transition metals such as Mn and Fe, owing to milder absorption effects at higher X-ray energies.

4. Results

Synthetic fluid inclusion samples containing NaCl–$CaCl_2$–H_20 (Vanko et al., 1988), $CaCl_2$–H_2O and KCl–H_2O were analyzed to assess the accuracy of the Ca/Cl and K/Cl determinations. One hundred and seventy four spectra from 82 inclusions having 15 different compositions in NaCl–$CaCl_2$–H_2O and $CaCl_2$–H_2O were obtained. Each spectrum was fit and the Cl and Ca peak intensities were tabulated as background-corrected integrated counts. Control spectra of nearby inclusion-free quartz were used to subtract any Cl or Ca counts not emanating from the inclusion itself (e.g., secondary fluorescence of nearby or underlying inclusions), and then the Ca/Cl ratio was calculated according to Eq. 4.

By far, the poorest agreement between calculated and nominal Ca/Cl ratio was for inclusions that were deep and, therefore, had small Cl peaks. Two spectra of inclusions with identical compositions, but at different depths in the quartz (Fig. 4), illustrate the strong depth

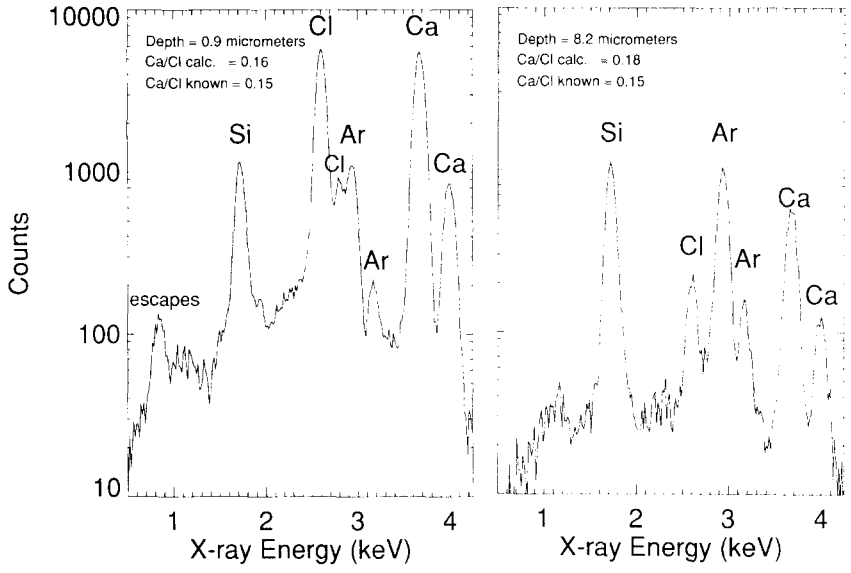

Fig. 4. Two spectra obtained from synthetic NaCl–$CaCl_2$–H_2O inclusions, one of which (on the left) is about 6 μm×6 μm in cross-section, and the other of which is about 9 μm×4 μm. Note the strong Cl and Ca peaks derived from the fluid. These inclusions have identical compositions, so the differences in relative Cl and Ca peak heights are due to differences in inclusion depth and mass.

control on the intensity of X-ray peaks. For the shallow inclusion, the Cl and Ca peaks exceed the Si and Ar peaks, and Cl is as intense as Ca. For the deeper inclusion, the Cl and Ca peaks are differentially absorbed. As an arbitrary, practical cut-off, we rejected spectra for inclusions greater than 14 μm deep or for inclusions whose control spectrum contained Cl at > 30% of that in the inclusion spectrum. Spectra obtained using a coarse beam (21×24 μm) were rejected in favor of those obtained with a fine beam (10×15 μm) because the former contained overwhelming Si and Ar counts compared to counts from the inclusion contents. The resulting 54 spectra show that Ca/Cl is analyzed with an uncertainty which is generally < ±30% (Table 1; Fig. 5).

Two synthetic inclusion samples with 20 and 36 wt% KCl in the system KCl–H_2O were investigated. Thirteen spectra require Cl background corrections less than 15% (the cut-off chosen for this element ratio), and for these the K/Cl ratio was calculated (Table 2). The average ratio is 1.18, compared to the known ratio of 1.10. This result is impressive because: (a) both K and Cl generate relatively soft X-rays, which are highly absorbed before they reach the detector, but also (b) both are affected by the large Ar peak with Cl on the low-energy shoulder and K on the high-energy side, overlapping strongly the Ar-K_β peak.

From the results in Tables 1 and 2, combined with laboratory notes on experimental conditions and archive photographs of each inclusion studied, the following general observations were made:

(1) Repeat analyses of individual inclusions, even on different days and different visits to BNL, commonly demonstrate excellent reproducibility (e.g., five spectra of inclusion *12-12-2* have calculated Ca/Cl from 0.133 to 0.184, average 0.147; compared to the known ratio of 0.15).

(2) Some analyses are very reproducible but differ from the nominal value (e.g., inclusions *3.0-1-1*, *3.0-1-2*, *3.0-2-1*, *3.0-2-2*, *6.5-6-3*, *6.5-6-6*). The most likely explanation is that the measured depth is incorrect. In each case the

TABLE 1

Results of Ca/Cl ratio determinations

Spectrum	Inclusion	Depth (μm)	Ca/Cl		% Difference	Spectrum	Inclusion	Depth (μm)	Ca/Cl		% Difference
			known	calculated					known	calculated	
80.73	*1-1-1*	12.0	0.12	0.068	−43	*81.26*	*9-1*-b	4.2	0.36	0.463	29
80.74	*1-1-1*	12.0	0.12	0.095	−21	*99.03*	*3.0-1-1*	6.8	0.565	0.764	35
80.75	*1-3-7*	8.0	0.12	0.074	−38	*99.12*	*3.0-1-1*	6.8	0.565	0.643	14
80.76	*1-3-7*	8.0	0.12	0.085	−29	*99.13*	*3.0-1-2*	5.7	0.565	0.388	−31
80.77	*1-3-7*	8.0	0.12	0.098	−18	*99.11*	*3.0-1-2*	5.7	0.565	0.442	−22
81.23	*11-9-3*	8.3	0.21	0.228	8	*100.12*	*3.0-1-2*	5.7	0.565	0.397	−30
81.09	*12-12-1*	6.2	0.15	0.184	23	*99.14*	*3.0-2-1*	7.4	0.565	0.320	−43
81.12	*12-12-2*	8.2	0.15	0.133	−11	*100.13*	*3.0-2-1*	7.4	0.565	0.308	−45
81.10	*12-12-2*	8.2	0.15	0.140	−7	*99.15*	*3.0-2-2*	7.3	0.565	0.631	12
81.11	*12-12-2*	8.2	0.15	0.141	−6	*100.14*	*3.0-2-2*	7.3	0.565	0.616	9
81.13	*12-12-2*	8.2	0.15	0.136	−10	*100.15*	*3.0-2-3*	6.9	0.565	0.496	−12
81.07	*12-12-2*	8.2	0.15	0.184	23	*100.17*	*4.0-10-14*	3.1	0.565	0.705	25
81.15	*12-13-6*	0.9	0.15	0.157	5	*100.10*	*4.0-10-3*b	7.7	0.565	0.507	−10
81.14	*12-13-6*	0.9	0.15	0.161	7	*99.72*	*4.0-10-7*	6.2	0.565	0.868	54
80.91	*3-5-4*	6.9	0.05	0.059	18	*99.73*	*4.0-10-8*	4.6	0.565	0.485	−14
80.81	*4-6-1*	4.2	0.04	0.053	32	*99.74*	*4.0-10-9*	4.9	0.565	0.624	10
80.84	*4-6-1*	4.2	0.04	0.045	12	*99.04*	*6.5-6-1*	13.9	0.565	0.476	−16
80.82	*4-6-2*	6.2	0.04	0.059	47	*99.09*	*6.5-6-1*	13.9	0.565	0.449	−21
80.94	*5-7-1*	2.8	0.26	0.758	191	*99.10*	*6.5-6-2*	8.5	0.565	0.510	−10
80.95	*5-7-2*	0.9	0.26	0.519	100	*99.07*	*6.5-6-2*	8.5	0.565	0.549	−3
80.98	*5-7-4*	11.4	0.26	0.270	4	*99.08*	*6.5-6-3*	6.9	0.565	0.424	−25
81.28	*6-3-1*	8.0	0.19	0.091	−52	*99.06*	*6.5-6-3*	6.9	0.565	0.428	−24
81.29	*6-3-1*	8.0	0.19	0.095	−50	*100.11*	*6.5-6-4*	6.9	0.565	0.511	−10
81.32	*6-3-3*	9.4	0.19	0.182	−4	*99.79*	*6.5-6-6*	7.7	0.565	0.446	−21
81.01	*8-8-1*	11.0	0.1	0.088	−12	*99.77*	*6.5-6-6*	7.7	0.565	0.411	−27
81.02	*8-8-2*	2.9	0.1	0.171	71	*99.78*	*6.5-6-7*	13.1	0.565	0.412	−27
81.25	*9-1-1*	1.5	0.36	0.402	12	*99.80*	*6.5-6-7*	13.1	0.565	0.330	−42

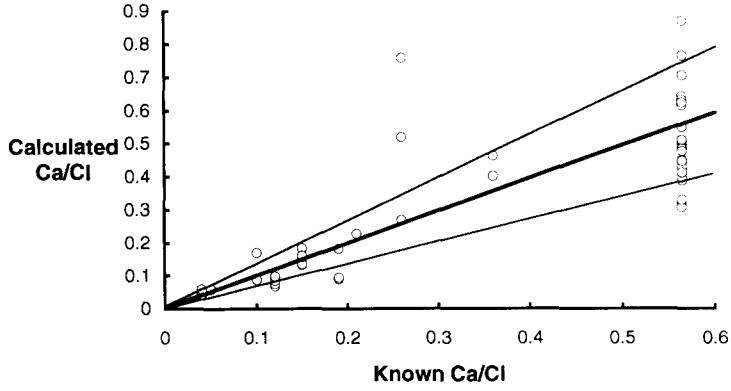

Fig. 5. Calculated vs. known Ca/Cl ratio for synthetic inclusions with various compositions in $NaCl–CaCl_2–H_2O$ and $CaCl_2–H_2O$, with a 1:1 line and the ±30% envelope drawn for comparison.

discrepancy can be explained by a depth uncertainty of only ~ ±1–1.5 μm.

(3) Inclusions that are larger than the microprobe beam cannot be analyzed because they are heterogeneous (especially brines with daughter crystals). Ideally, the X-ray beam

TABLE 2

Results of K/Cl ratio determinations

Spectrum	Inclusion	Depth (μm)	K/Cl		% Difference
			known	calculated	
102.52	*20-1-1*	10.5	1.103	0.866	−21
102.53	*20-1-2*	2.5	1.103	1.089	−1
102.56	*20-1-4*	6.0	1.103	1.315	19
102.60	*20-1-8*	0.3	1.103	1.565	42
102.61	*20-1-9*	7.9	1.103	0.834	−24
102.62	*20-2-1*	4.0	1.103	1.691	53
102.63	*20-2-2*	5.6	1.103	1.059	−4
102.13	*36-1-4*	3.9	1.103	1.034	−6
102.19	*36-1-4*	3.9	1.103	1.012	−8
102.16	*36-1-5*	7.3	1.103	1.063	−4
102.40	*36-2-1*	3.7	1.103	1.421	29
102.42	*36-2-1*	3.7	1.103	1.357	23

should irradiate the whole inclusion, with no overlap of neighboring (either laterally or underneath) inclusions. All spectra in Table 1 are from inclusions less than ~ 12 μm across.

(4) Inclusions with irregular shapes, especially those that plunge down away from the surface, are difficult to analyze accurately because a single depth value is inappropriate.

(5) Fine beam analyses are better than those using a broad beam. Although the broad beam produces much higher count rates for Ca and Cl, it also floods the spectrum with more Si and Ar counts and the Cl–Ar overlap becomes intractable.

5. Discussion and conclusion

In this study we have detected light X-rays from Cl, Ca and K quantitatively using SXRF, and have used these data to calculate Ca/Cl and K/Cl ratios. These elements, along with Na, comprise the major elements in most aqueous fluid inclusions. The SXRF method can both confirm the choice of chemical system used to model microthermometric data, and can provide quantitative values for individual inclusions. With careful, conservative choices of the inclusions to be examined, elemental ratios of Ca/Cl and K/Cl are accurate to $\pm$10–30%. This result is strictly applicable only to concentrated brine inclusions: low-salinity inclusions are more difficult to analyze primarily because of background fluorescence from the host.

Future improvements may allow the accuracy of the analyses presented in this study to be improved significantly. Use of a wavelength-dispersive detector would allow better resolution between the Ar peak and the adjacent Cl and K peaks. Placing the experiment in a vacuum or a He atmosphere would eliminate the Ar peak altogether. Finally, next generation synchrotrons such as the Advanced Photon Source (being constructed at Argonne National Laboratory) will generate X-rays with several orders of magnitude greater flux allowing the counting statistics for light elements to be improved significantly.

Because the K_α X-rays of transition and other heavy trace elements are not as strongly absorbed by the host mineral, future SXRF analyses involving these elements are expected to yield more precise results than for the light elements described here. The inclusions that can be analyzed for these elements can be slightly deeper [of the order of several tens of micrometers (Frantz et al., 1988; Rankin et al., 1992)].

In conclusion, SXRF experiments with synthetic fluid inclusions have demonstrated the accuracy of the technique for Ca/Cl and K/Cl determinations. Used in concert with microthermometric studies, SXRF should prove to be invaluable in approaching the goal of all fluid inclusion studies: a comprehensive chemical analysis of the bulk natural fluid.

Acknowledgements

This study was supported by the National Science Foundation (EAR-9103530 and OCE-9114832 to D.A.V., EAR-8915699 to M.L.R., EAR-8657778 to R.J.B.), the National Aeronautic and Space Administration (NAG9-106 to SRS) and the U.S. Department of Energy (DE-AC02-76CH00016). Some of the synthetic inclusions were prepared in the Fluids Research Laboratory at Virginia Tech by Charlie Oakes under U.S. Department of Energy contract DE-FG05-89ER14065 to R.J.B. We thank Keith Jones and the rest of the NSLS staff at X26A for their assistance, and the NSLS User Administration for logistical and partial travel support for D.A.V. Georgia State University provided seed funds in the form of a GSU Research Grant (91-015). We also thank colleagues who assisted in data collection or provided stimulating discussions about this project: Andy Campbell, Ed Roedder, Mo Ghazi, Tim LaTour and Phyllis Midkiff. Thanks are also extended to journal reviewers Phil Brown and Jim Irwin for many helpful suggestions.

References

Bassett, W.A. and Brown, Jr., G.E., 1990. Synchrotron radiation: Applications in the earth sciences. Annu. Rev. Earth Planet. Sci., 18: 387–447.

Bodnar, R.J. and Sterner, S.M., 1987. Synthetic fluid inclusions. In: G.C. Ulmer and H.L. Barnes (Editors), Hydrothermal Experimental Techniques. Wiley, New York, N.Y., pp. 423–457.

Chen, J.R., Chao, E.C.T., Minkin, J.A., Black, J.M., Bagby, W.C., Rivers, M.L., Sutton, S.R., Gordon, B.M., Hanson, A.L. and Jones, K.W., 1987. Determination of the occurrence of gold in an unoxidized Carlin-type ore sample using synchrotron radiation. Nucl. Instrum. Methods Phys. Res., B22: 394–400.

Chen J.R., Chao, E.C.T., Minkin, J.A., Black, J.M., Jones, K.W., Rivers, M.L. and Sutton, S.R., 1990. The uses of synchrotron radiation sources for elemental and chemical microanalysis. Nucl. Instrum. Methods Phys. Res., B49: 533–543.

Criss, J., 1977. NRLXRF, Naval Research Laboratory Cosmic Program #DOD-00065. Naval Res. Lab., Washington, D.C.

Flynn, G.J. and Sutton, S.R., 1992. Trace elements in chondritic stratospheric particles: zinc depletion as a possible indicator of atmospheric entry heating. Proc. 22nd Lunar Planet. Sci. Conf., pp. 171–184.

Frantz, J.D., Mao, H.K., Zhang, Y.-G., Wu, Y., Thompson, A.C., Underwood, J.H., Giauque, R.D., Jones, K.W. and Rivers, M.L., 1988. Analysis of fluid inclusions by X-ray fluorescence using synchrotron radiation. Chem. Geol., 69: 235–244.

Kopp, O.C., Reeves, D.K., Rivers, M.L. and Smith, J.V., 1990. Synchrotron X-ray fluorescence analysis of zoned carbonate gangue in Mississippi Valley-type deposits (U.S.A.). Chem. Geol., 81: 337–347.

Lowenstern, J.B., Mahood, G.A., Rivers, M.L. and Sutton, S.R., 1991. Evidence for extreme partitioning of copper into a magmatic vapor phase. Science, 252: 1405–1409.

Lu, F.-Q., Smith, J.V., Sutton, S.R., Rivers, M.L. and Davis, A.M., 1989. Synchrotron X-ray fluorescence analysis of rock-forming minerals, 1. Comparison with other techniques; 2. White-beam energy-dispersive procedure for feldspars. Chem. Geol., 75: 123–143.

Rankin, A.H., Ramsey, M.H., Coles, B., Van Langevelde, F. and Thomas, C.R., 1992. The composition of hypersaline, iron-rich granitic fluids based on laser–ICP and synchrotron–XRF microprobe analysis of individual fluid inclusions in topaz, Mole granite, eastern Australia. Geochim. Cosmochim. Acta, 56: 67–79.

Rivers, M.L., Sutton, S.R. and Jones, K.W., 1991. Synchrotron X-ray fluorescence microscopy. Synchrotron Radiat. News, 4: 23–26.

Roedder, E., 1990. Fluid inclusion analysis — Prologue and epilogue. Geochim. Cosmochim. Acta, 54: 495–507.

Sutton, S.R. and Flynn, G.J., 1990. Extraterrestrial halogen and sulfur content of the stratosphere. Proc. 20th Lunar Planet. Sci. Conf., pp. 357–362.

Sutton, S.R., Delaney, J., Smith, J.V. and Prinz, M., 1987. Copper and nickel partitioning in iron meteorites. Geochim. Cosmochim. Acta, 51: 2653–2662.

Treiman, A.H. and Sutton, S.R., 1992. Pyroxenes in the Zagami Shergottite: Chemical zoning by synchrotron X-ray (SXRF) microprobe and electron microprobe and implications for petrogenesis. Geochim. Cosmochim. Acta, 56: 4059–4074.

Vanko, D.A., Bodnar, R.J. and Sterner, M.A., 1988. Synthetic fluid inclusions, VIII. Vapor-saturated halite solubility in part of the system $NaCl-CaCl_2-H_2O$, with application to fluid inclusions from oceanic hydrothermal systems. Geochim. Cosmochim. Acta, 52: 2451–2456.

White, R.N., Smith, J.V., Spears, D.A., Rivers, M.L. and Sutton, S.R., 1989. Analysis of iron sulphides from UK coal by synchrotron radiation X-ray fluorescence. Fuel, 68: 1480–1486.